Comparison of a Piecewise Transformation to Polynomial-Based Geometric Correction Algorithms

Heidi Ochis, Computer Terrain Mapping, Inc., Boulder, CO.
Edward C. Russell, Computer Terrain Mapping, Inc., Boulder, CO.

Abstract

A major factor restricting the usefulness of digital aerial photography as a GIS thematic layer has been the limited ability of polynomial-derived transformation equations to remove displacements caused by non-uniform terrain relief. A piecewise transformation algorithm, which uses Delaunay triangles, was developed which geographically "anchors" all ground control points and transforms the imagery on a triangle by triangle basis. This algorithm was compared to three polynomial-derived least squares regression transformation algorithms on a digital aerial photograph with non-uniform image displacements. The test image has been divided into two sections which represent hilly terrain (large image displacements) and relatively flat terrain (small image displacements). The evaluation compares each algorithm's relative geographic accuracy on the two sections individually and on the image as a whole. The evaluation also compares each algorithm's relative geometric accuracy as the number of rectification control points are incrementally increased on the total image.

The piecewise algorithm produced significantly more accurate transformations than any of the polynomial transformations in the mountainous section and overall image. In the flat section, the piecewise algorithm was significantly more accurate than the first order transformation and slightly more accurate than 2nd and 3rd order transformations. The piecewise transformation performed better than all polynomial-based transformations for all incremental tests. The piecewise algorithm, the methodology for testing the accuracy of each algorithm, and the results of the comparisons are described and discussed.

Introduction

Using digital imagery as a thematic layer is important in many GIS applications (Nale, 1996, Green, 1992). These images supply information on vegetation, geomorphology and general landscape patterns not available by sources other than ground surveys. Geographically rectifying these images to correctly match local roads, streams and political boundaries is key to their usefulness as integrated GIS layers.

With planimetric maps, all features are located in their correct horizontal positions and are depicted as though they were being viewed from directly overhead. Because aerial imagery views all objects from a single point (perspective projection), many ground objects are shifted or displaced from their correct positions. This phenomenon is known as image displacement. The most significant source of image displacement is topographic relief (Avery and Berlin, 1992).

Ideally, all digital imagery used in a GIS database would be orthorectified, resulting in a digital orthophoto. Digital orthophotos are digitally reconstructed photographs that shows natural and cultural features in their true planimetric positions. All geometric distortions and relief displacements are removed from the standard perspective photographs. Two main sources of input data are required: a digitized aerial photograph and a digital elevation model (DEM). In addition, several other parameters are needed. These consist of target and image coordinates of ground control points, camera calibration information, and photograph fiducial coordinates in the raster image (Hood, 1989). Unfortunately the list of additional data needed to execute an orthorectification is not available for many photos. Also, as discussed by Novak (1992), and Hood (1989), because the ortho-image is mapped to the DEM, the accuracy of the target image (orthophoto) is primarily limited by the accuracy and resolution of the DEM. Two types of alternative rectification methods are described which can be used when adequate information for an orthorectification is absent.

The most common methods for geo-rectifying digital imagery are the least squares regression transformations which utilize low order polynomial surfaces. Depending upon the severity of displacement in the imagery and the number of ground control points available, complex polynomial equations may be used to express the transformation. Because these equations are based on global functions of x and y, they work well for photographs with quasi-uniform displacements. First order transformations perform well for photographs with little change in the overall image displacement while second and third order transformations may work well for photographs with a limited amount of relatively smooth and uniform change in the overall image displacement. Because polynomials are best fit equations for an entire image, they may not compensate adequately for significant local displacements. Therefore these transformations are limited in their ability to model and thus remove non-uniform or abrupt local displacements (Figure 1a-c).

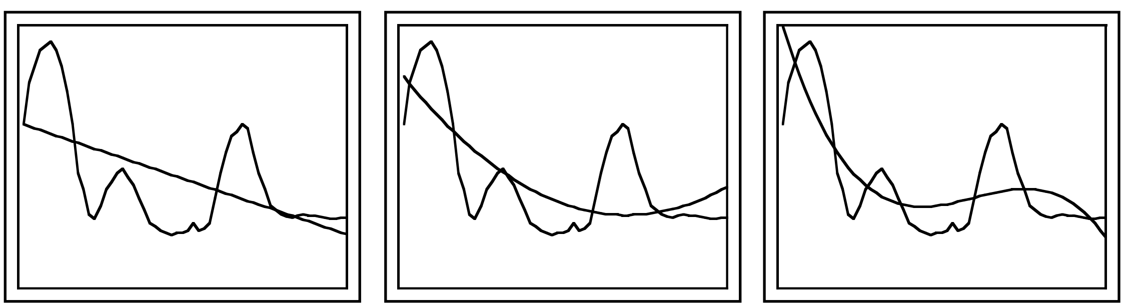

1.a 1.b 1.c

Figure 1. Best fit polynomial equation lines for a hypothetical displacement surface: a) First order polynomial, b) second order polynomial, c) third order polynomial.

Another rectification option is a piecewise transformation. Piecewise transformations reconstruct the digital images in “patches” between ground control points (GCPs). These patches are typically triangles that form an irregular mesh covering most or all of the image (Figure 2). The

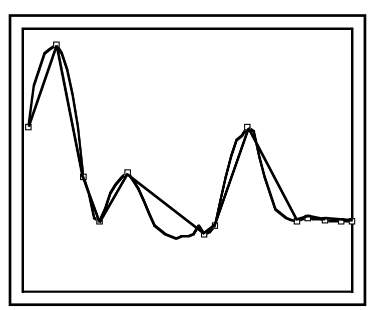

Figure 2. Best fit piecewise transformation triangulation for a hypothetical displacement surface.

transformation of the image is then executed on a triangle by triangle basis. A GCP exerts influence only on those triangles in which it is a vertex. While each triangle will have a different transformation function, adjacent triangles will share the same transformation function values at their common edge. This makes the piecewise transformation continuous across the image so that the transition from one triangle to another becomes seamless.

This study introduces a piecewise transformation and compares it to more traditional rectifications procedures. The geographic accuracy of polynomial based transformations (specifically 1st, 2nd and 3rd order) and the piecewise transformation are analyzed on an image representing non-uniform terrain / displacements.

Previous Work

Devereux, et al (1990) used a triangulation based rectification for airborne multi-spectral scanner (AMSS) imagery. Their procedure used a Delaunay triangulation of control points in the image and target space. The image and target triangles were then matched and a best fit linear transformation was calculated for each triangle pair.

Chen and Rau (1993) took a similar approach as Devereux, et. al (1990). They used an existing orthophoto generated from aerial photographs to collect GCP data for an AMSS image. After the GCPs were selected, the Delaunay triangulation was generated. For each triangle, a transformation of the coordinates for each image pixel to the reference system was calculated using the a best fit linear transformation according to the three vertices of the triangle pair.

PCI™ (Thin Plate Splines) and Vector Vision™(Image Positioning System) software each provide a form of piecewise transformation as a geo-rectification option. These software packages are proprietary, so descriptions of the algorithms are not available for comparison. Therefore the performance and mechanics of the piecewise transformation described here are not necessarily a description of the commercial versions.

TRANSFORMATIONS TO BE COMPARED

Polynomial Transformations

Perhaps the most common method for georectifying digital imagery is the least squares regression transformation utilizing a low order polynomial surface. The procedure commonly followed is to locate ground control points (GCPs) in terms of both their image coordinates (column, row) and reference coordinates (UTM, latitude and longitude, etc.). These values are then submitted to a least squares regression analysis to determine coefficients for two transformation equations that interrelate the target (or geographic) and image coordinates:

$$u = \sum_{i=0}^{n} \sum_{j=0}^{i} a_k x^{i-j} y^j \qquad v = \sum_{i=0}^{n} \sum_{j=0}^{i} b_k x^{i-j} y^j$$

(Equation 1) (Equation 2)

where :

$$k = \frac{i\,(i+1)}{2} + j$$

(x,y) = target coordinates (column, row) (u,v) = image coordinates
a_k, b_k = equation coefficients n = the order of the polynomial

For example:

for n = 1 $u = a_0 + a_1x + a_2y,$
$v = b_0 + b_1x + b_2y$

for n = 2 $u = a_0 + a_1x + a_2y + a_3x^2 + a_4xy + a_5y^2,$
$v = b_0 + b_1x + b_2y + b_3x^2 + b_4xy + b_5y^2$

The transformation can be either a forward mapping from image space to target space, or an inverse mapping from target space to image space. Equations 1 and 2 describe an inverse mapping process. Each desired location in the target space is “visited” and transformed to an image coordinate. The image pixels surrounding this coordinate are used to interpolate the intensity for the target location. Some common intensity interpolation methods are nearest neighbor, bilinear, and cubic convolution.

Depending upon the displacement in the imagery and the number and distribution of GCPs used, complex polynomial equations may be required to express the needed transformation. The degree of complexity of the polynomial is expressed as the order of the polynomial, which is simply the highest exponent used in the polynomial equation.

Transformations of 2nd order or higher are non-planar. These can compensate for non-planar displacements which are fairly uniform in nature. As the complexity of the displacement increases, the order of the transformation may need to be increased. But, by increasing the order of the polynomial for the sake of achieving a best fit equation for all GCPs, the equation may become more complex than necessary, causing unwanted displacement in areas with no GCPs in the output image.

Piecewise Transformation

The piecewise transformation presented here works in three major steps. It first computes the Delaunay tessellation from a set of control points (detailed below), then it establishes the image - target transformation parameters, and finally it interpolates the intensity of each pixel in the transformed file.

Delaunay Tessellation. Using an algorithm from D. F. Watson (1982), the piecewise transformation computes the Delaunay tessellation (tiled triangulation) from a set of control points. This produces triangles whose interior angles are as near to equal as possible, so as to avoid thin and long triangles (Sibson, 1978, O’Hair, 1978). It also guarantees the same triangulation will be produced from a given data set, regardless of the starting point for the triangulation construction.

For image rectifications, a process for handling cells that lie outside the region (convex hull) of the triangulation should be addressed. McCullagh and Ross (1980) suggested the most efficient method for solving a triangulation boundary problem is to place a set of imaginary points around the outside of the area, just beyond the data window. However, the imaginary points in a rectification must be paired with points in target space. The target coordinates for the imaginary points could be calculated in many ways. One option would be to use all true data points to create a trend surface (e.g. a polynomial transformation equation). The imaginary points could then be projected into the target space, and those coordinates used as the corresponding target pairs. Another possibility would involve extending the edge triangles to include the entire area of interest, using similar triangles. A logical method of choosing the most appropriate triangles to extend is problematic, however. Solving the triangulation boundary problem is worthy of further investigation. For this study, data points which fall outside the convex hull of the triangulation will be ignored for all transformations being compared.

Image to Target Transformation. The image - target transformation in the piecewise algorithm uses a technique described by O'Hair (1978). The technique provides a method for locating a point in a Delaunay triangulation. Each point location can be calculated with respect to the triangle by solving Equations 3 - 5 for **r** = (r1,r2,r3). The three values, r1, r2, and r3, indicate whether the point is within, on the boundary, or outside the triangle and control the degree of influence of each of the triangle vertices (Figure 3).

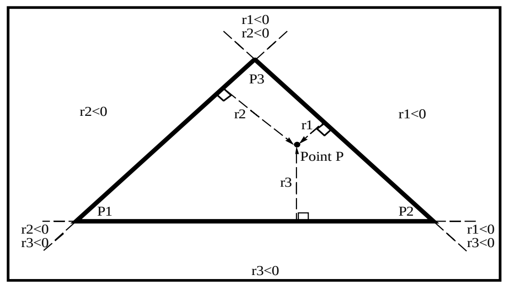

Figure 3. Illustrates the values of . The three components of **r** always sum to 1; when all the values are positive, the point is inside the triangle. Point P's location can be calculated using the scaling values of r1, r2 and r3 and the coordinates P1, P2 and P3.

For example, suppose a triangle has vertices P1, P2, P3 with corresponding image space coordinates of (u1,v1), (u2,v2), (u3,v3) and target space coordinates (x1,y1), (x2,y2), (x3,y3). For a point P within the triangle, with target space coordinate (x,y), the corresponding image space coordinate (u,v) is found by solving:

$$\mathbf{x} = \mathbf{Ar} \qquad \text{(Equation 3)}$$

where:

$$\mathbf{x} = \begin{bmatrix} x \\ y \\ 1 \end{bmatrix} \qquad \mathbf{A} = \begin{bmatrix} x1 & x2 & x3 \\ y1 & y2 & y3 \\ 1 & 1 & 1 \end{bmatrix} \qquad \mathbf{r} = \begin{bmatrix} r1 \\ r2 \\ r3 \end{bmatrix}$$

for **r**: $$\mathbf{r} = \mathbf{A}^{-1}\mathbf{x} \qquad \text{(Equation 4)}$$

with **r** from equation 4: $$\mathbf{u} = \mathbf{Br} \qquad \text{(Equation 5)}$$

where:

$$\mathbf{u} = \begin{bmatrix} u \\ v \end{bmatrix} \qquad \mathbf{B} = \begin{bmatrix} u1 & u2 & u3 \\ v1 & v2 & v3 \end{bmatrix}$$

The transformation outlined in equation 3 - 5 is an inverse mapping. As described in the previous section, once the transformation equation has been solved an interpolation method is used to determine an output intensity value.

METHODOLOGY FOR ACCURACY ASSESSMENT

Study Photograph

In order to test each rectification algorithm, a U. S. Geological Survey (USGS) National Aerial Photography Program (NAPP) photo of the Lyons, Colorado area was used. This photograph covers an area that contains significant elevation change (i.e., ~500m) in its western portion. The image was digitally scanned so that each pixel represented 3.5 meters on the ground.

In order to test each rectification algorithm on images which represent quasi-uniform and non-uniform displacement effects, the image was divided into 2 sections: east and west. Each section, by itself, represents relatively uniform terrain. The eastern half has little terrain relief, resulting in quasi-uniform image displacements, while the western section has high relief terrain, also resulting in quasi-uniform image displacements. By using the entire image, the image displacements become non-uniform. Figure 4a illustrates the image division in 3 dimensions. The point distribution is plotted in Figure 4b**.**

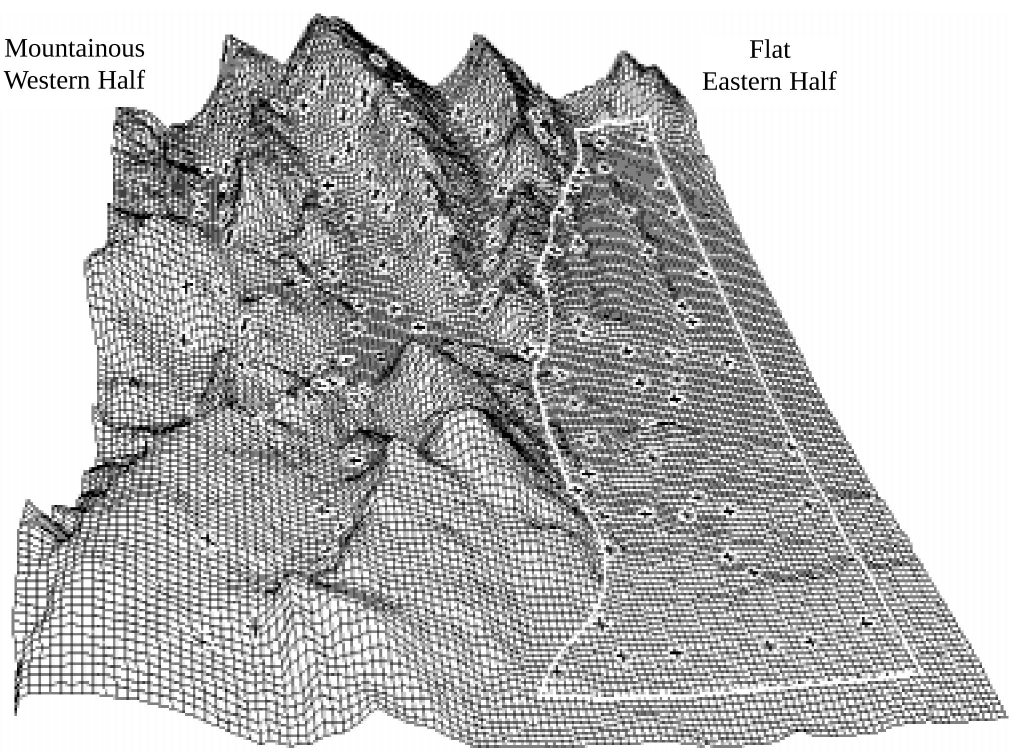

Figure 4a. Image division and point distribution draped over a 3D model of study area. The white line indicates the image division.

Point selection

To avoid “clusters” of ground control points, the photograph was divided into 176 equally sized cells. Each cell was examined for a potential ground control point. Because of private property issues or lack of identifiable features, a total of 131 points out of the potential 176 were collected. The large area in the lower center of the image contained no data points due to property access problems and the lack of identifiable features due to snow coverage. All points were collected using a Trimble Pathfinder Basic™ Plus receiver by driving, hiking or biking to the identified locations.

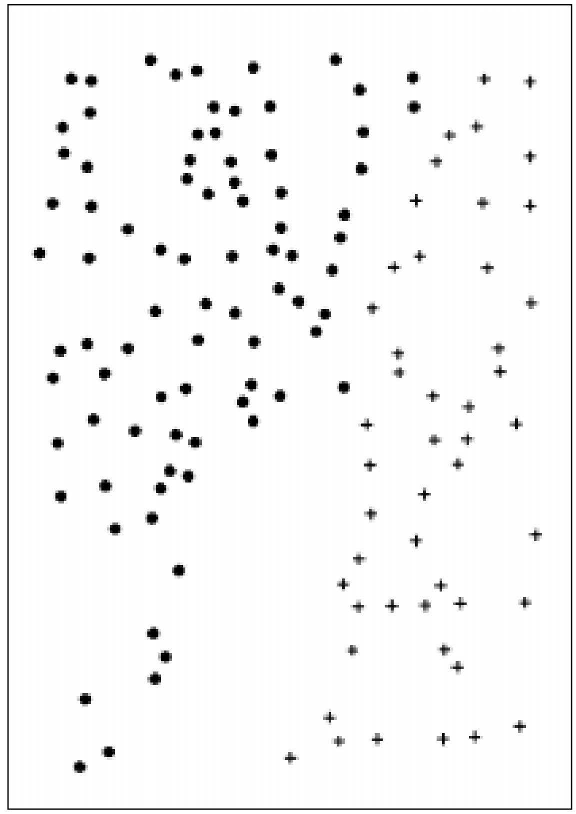

Figure 4b. GCP point distribution in plan view of the study area. The + points are the GCPs in the flat section and the • points are the GCPs in the mountainous section.

At each GCP position, at least 180 readings were collected at 3 seconds intervals, then differentially corrected using PFINDER™ software (Brown, 1996, Votava, 1996). The 180 corrected readings were then averaged into a single geographic location.

All post-processing utilized the Trimble community base station, operated by the USDA Forest Service in Ft. Collins. The study site falls well within the 300 mile range suggested by Trimble for base station data collection (Trimble Navigation, Ltd., 1992). After differential correction and averaging, the resulting GCPs should have better than 2 meter horizontal accuracy.

Testing constraints

In establishing a methodology for testing the accuracy of each transformation, several factors needed consideration. First, the piecewise transformation “anchors” the control points. That is, the transformed pixel located at a control point matches the reference value exactly. In general, this is not the case with the polynomial surfaces: control points influence the value of the transformed pixel control point, but do not fully determine it. The accuracy of a polynomial transformation is usually estimated by the root mean squared error (RMSE) between the reference control points and the transformed pixels located at the control points. Obviously, this method of estimating accuracy would be strongly biased toward the piecewise transformation which would have a zero RMSE.

Second, the piecewise transformation described earlier operates only within the convex hull of the Delaunay triangulation. While there are several possible methods of extending this to cover the entire image, these methods would produce their own forms of error. Consequently, error estimation has been limited to the triangulation region.

Finally, since the accuracy assessment is to occur only within the convex hull of the control points, it is important to keep the points which make up the convex hull constant so that points will not "fall out" of the triangulation by changing the point configuration of the outer edge. This has an affect on which points are to be used as accuracy check points.

Methodology

Because of the constraints mentioned above, a cross-validation approach was used to evaluate the accuracy of each transformation algorithm. This approach is similar to the method used by McGwire (1996). Instead of performing the transformation using all the control points, the cross-validation method uses an iterative sample substitution and calculation to create check points which are independent from the corresponding transformation coefficients. The procedure for the accuracy evaluation follows.

First, a triangulation is generated using all possible GCPs in order to identify the points which make up the "outer edge" or convex hull of the triangulation. Those points are then used in all transformation calculations (detailed below). From the remaining interior points, one control point is removed from the pool of GCPs. The geometric transformation is then calculated using the remaining points. That transformation is then applied to the removed point and its difference from the true value is calculated. The removed point is then placed back in the GCP pool and the process is applied iteratively to each point that falls in the interior of the triangulation.

Every exterior point is kept as a GCP only, in order to avoid a triangulation configuration which excludes that point. If the point falls outside the convex hull, there is no transformation equation available for that point, making an error calculation unachievable. Figure 5 illustrates this situation. By calculating error values for interior points only, the number of tested points stayed constant between the algorithms.

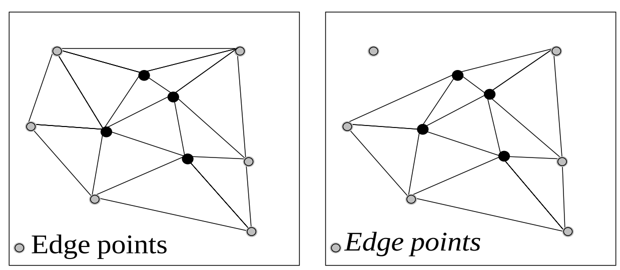

Figure 5. Rationale for identifying "edge" points and using them for GCP locations only. If the edge points were removed from the geometric transformation calculation to be used as a check point, there is a high probability the point would fall outside the triangulation in the case of the piecewise transformation thus making an error calculation unachievable.

Each algorithm was also tested with an increasing number of control points to evaluate how the geometric accuracy was affected. To gauge algorithm performance with increasing numbers of control points, test sets of 40, 50, 60, 70, 80, 90, 100, 110, 120 and 131(all) control points were used. The methodology for choosing points within each increasing test set is described next.

The tests started with 40 points which were made up of the 20 edge points plus 20 randomly chosen points. The points were incrementally increased by 10 until all the control points were used.

The first 20 randomly chosen points were the only points used as check points for every subsequent incremental test. This was done to avoid the introduction of unaccounted for error with the addition of new points to the check point group.

The accuracy of a rectification was heavily dependent on the location of the control points chosen. If points were chosen in an area with large image displacements, the influence of those points would cause the overall image error to be higher than if they were not chosen. For example if the first set of 40 points contained control points with relatively low error, the average error would be relatively low. If in the next assessment group several of the added points had relatively high error, because they were from areas associated with large image displacements, the average error would actually increase. Table 1 demonstrates the variability in error associated with the check points by tabularizing the standard deviation, minimum and maximum control point errors.

In order to mitigate the effect points associated with high error have on a single rectification, the ideal solution would be to test every possible 20 point combination of control points out of the pool of 111 control points and look at the average error of all possible transformations using 20 points. Because the pool of control points used to choose the 20 point combinations was large (111 points), the number of calculations became unmanageable (111! / 20!(111-20)!). In addition, the process would have to be executed on each of the 50 through 131 point sets, so the number of calculations would be enormous. Due to time and resource limitations, this was not a practical option. As an alternative, 10 realizations were run at each increment using a different random point set for each realization.

To test the geometric accuracy of each rectification, the cross-validation method, described previously, was used. The initial 10 sets of 20 points chosen for use in the first incremental test were averaged to estimate an error associated with each algorithm. For each subsequent increase in points, the same test points were used. The rationale for testing the same 20 points for each increment was: 1) the number of points stays consistent and 2) the test evaluated the same 20 points each time so that uncontrolled error was not introduced from one incremental group to the next. This made the incremental comparisons easier to evaluate.

RESULTS AND CONCLUSIONS

Summary

The basis for a new piecewise approach to geometric corrections using Delaunay triangles has been described and evaluated against three polynomial-based correction algorithms. Each algorithm was tested on an image that contained quasi-uniform and non-uniform image displacements caused by terrain. By dividing the image, the algorithms were tested in a relatively flat area (i.e. quasi-uniform, relatively small image displacements), a mountainous area (again, quasi-uniform, but relatively large image displacements) and on the combined flat and mountainous areas (non-uniform image displacements).

The piecewise transformation presented in this study anchors all control points so that the transformed GCPs match their related reference values exactly, i.e. the image RMSE would equal zero if the control points used in the transformation were also used as check points. This is because the piecewise transformation uses the control points as triangle corners and transforms the image on a triangle by triangle basis. Therefore a methodology for testing the accuracy of the geometric transformations was used that removes the potential bias toward the piecewise transformation. A cross-validation procedure was used to test the accuracy of each rectification which was previously described above and by McGwire (1996).

The accuracy results are summarized in Table 1 and Figure 6. The piecewise transformation was significantly more accurate using a paired two sample t-test for means, at $\alpha=0.01$, in all cases except in the flat terrain where it was only slightly more accurate than the 2nd and 3rd order transformations.

Table 1. Summary of transformation results for all control points using the 1st order, 2nd order, 3rd order and piecewise transformation in the flat terrain, mountainous terrain and the total image.

flat area (east)	RMSE (meters)	*min (meters)*	*max (meters)*	*SD (meters)*	*No. of test pts*
TIN	*12.4*	*1.6*	*93.2*	*16.2*	*31*
1st	*18.8*	*6.1*	*105.4*	*16.9*	*31*
2nd	*14.4*	*5.0*	*105.0*	*17.3*	*31*
3rd	*14.1*	*1.9*	*95.7*	*16.0*	*31*
mtn. area (west)	RMSE (meters)	*min (meters)*	*max (meters)*	*SD (meters)*	*No. of test pts*
TIN	*13.6*	*0.9*	*75.6*	*12.2*	*68*
1st	*28.3*	*3.1*	*92.2*	*16.9*	*68*
2nd	*26.1*	*2.7*	*92.7*	*15.7*	*68*
3rd	*18.7*	*1.0*	*57.4*	*13.1*	*68*
total image	RMSE (meters)	*min (meters)*	*max (meters)*	*SD (meters)*	*No. of test pts*
TIN	*14.1*	*0.9*	*93.2*	*14.5*	*111*
1st	*31.2*	*2.0*	*131.7*	*25.5*	*111*
2nd	*24.3*	*1.4*	*104.6*	*18.2*	*111*
3rd	*19.6*	*1.8*	*81.5*	*15.4*	*111*

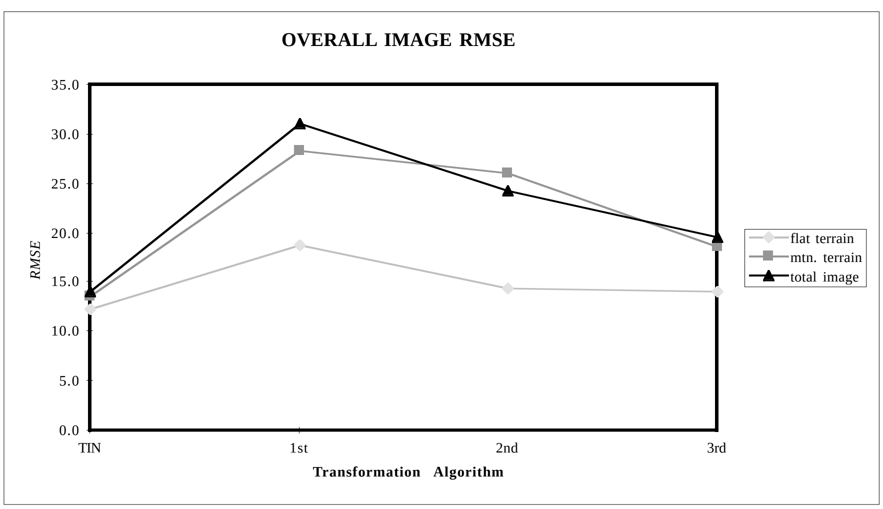

Figure 6. Graphic summary of the average RMSE for all control points using the 1st order, 2nd order, 3rd order and piecewise transformations in the flat terrain, mountainous terrain and total image.

Because the piecewise transformation is based on a triangulation of the available control points, it has the ability to represent the changes in displacement across an image more effectively than polynomial-based transformation which globally average the control points to calculate a best fit surface. This is especially true in images with non-uniform displacements.

Another objective of this study was to determine the impact of increasing the numbers of rectification control points on the geometric accuracy of each algorithm. A total of 20 test points were used to evaluate each algorithm using the cross-validation method. The piecewise transformation produced rectifications that were significantly more accurate at an a=0.01 than any of the polynomial-based rectifications at every increment. The average accuracy of each rectification algorithm generated with increasing numbers of control points are summarized in Figure 7.

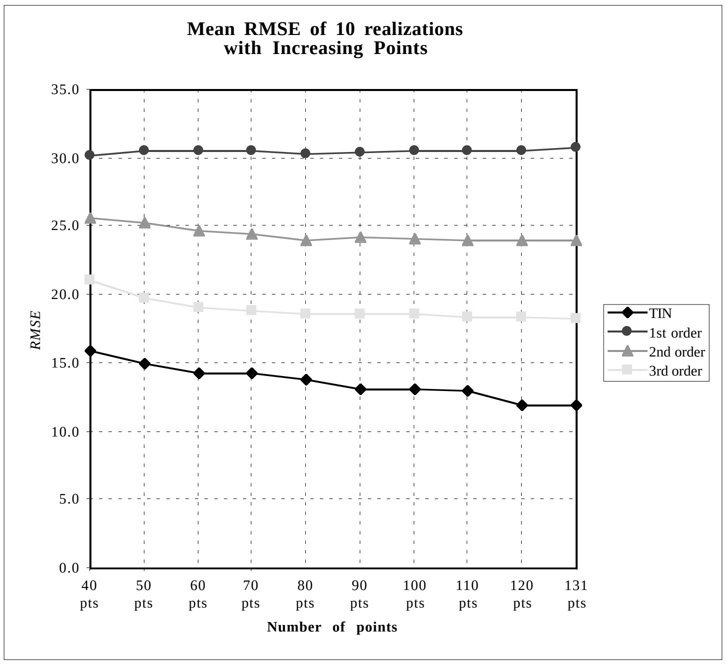

Figure 7. Graph of average RMSE for 10 realizations of 20 test points. Each rectification algorithm was tested in the total image with increasing numbers of control points.

Because of the severity of the displacement found in the image being rectified, the addition of control points was not necessarily beneficial to the polynomial-based transformations. Because these transformations calculate the best fit polynomial surfaces for x and y, the addition of control points associated with large displacements, would skew the resulting surfaces.

As a result the 1st order transformation never significantly improved in accuracy and in fact got worse. The 2nd and 3rd order transformations improved up to 50 pts for the 2nd order and 60 pts for the 3rd order after which no significant improvement occurred with the addition of control points.

The piecewise transformation, on the other hand, continued to significantly improved in accuracy with the addition of control points. With an infinite number of control points, the piecewise transformation would be expected to improve until the points used were located such that all the image displacements were accurately represented.

Identified shortcomings and recommendations for further research

A few problems were identified while using the piecewise transformation during this study and are described below.

Shortcoming. The piecewise transformation, as mentioned previously, is very sensitive to poorly placed GCPs. There is no easy solution to this problem other than to use the most accurate data available. Collecting GCP data using a GPS receiver can help reduce "bad" GCP data points, but can be very time consuming.

Research. The area of a photograph which falls outside the convex hull of the triangulation needs to be addressed. Currently, areas of an image that fall outside of the convex hull of a triangulation are simply lost when using a piecewise transformation. They are not transformed and are therefore clipped off. Using aerial imagery as a thematic layer often involves mosaicking several photographs together. In order to tile images effectively, the image edges need to match as closely as possible. In order to tile images together, the outer edge problem needs to be addressed.

The main objective of this study was to compare the accuracy of a triangle-based piecewise transformation to polynomial-based geometric correction algorithms. Under the tested conditions, the piecewise transformation appears to be a very powerful tool. This method has the capability to cope with complex patterns of displacement and in most cases performs significantly better than traditional polynomial-based methods for rectifying digital aerial images. It was found to be especially effective in rectifying imagery with non-uniform image displacements.

REFERENCES

Avery, T. E., and G. L. Berlin, 1992. *Fundamentals of Remote Sensing and Airphoto Interpretation,* Principles of Photogrammetry, 5th ed., New York: Macmillan Publishing Co., pp. 71-77.

Chen, L. C. and J. Y. Rau, 1993. Geometric correction of airborne scanner imagery using orthophotos and triangulated feature point matching. *International Journal of Remote Sensing,* 14(16):3041-3059.

Devereux, B. J., R. M. Fuller, L. Carter, and R. J. Parsell, 1990. Geometric correction of airborne scanner imagery by matching Delaunay triangles. *International Journal of Remote Sensing*, 11(12):2237-2251.

Green, Kass, 1992. Spatial Imagery and GIS. Integrated data for natural resource management. *Journal of Forestry*, 90(11): 32-36 .

Hood, Joy, Lyman Ladner, and Richard Champion, 1989. Image Processing Techniques for Digital Orthophotoquad Production. *Photogrammetric Engineering & Remote Sensing*, 55(9):1323-1329.

McCullagh, Michael J., and Charles G. Ross, 1980. Delaunay triangulation of a random data set for isarithmic mapping. *The Cartographic Journal*, 17(2):93-99.

Nale, David K., Thurgood, Jolyon D., 1996. Integrating Space-Based Imagery with GIS Landbase Datasets. *GIS World*, 9(6):58.

Novak, K., 1992. Rectification of Digital Imagery. *Photogrammetric Engineering & Remote Sensing*, 58(3):339-344.

O'Hair, Kelly, 1978. Contours from irregular data points. Lawrence Livermore Laboratory document. UCID-30170, Computer documentation. Prepared for US Energy Research & Development Administration under contract No. W-7405-Eng-48.

Sibson, R., 1978. Locally equiangular triangulations. *Computing Journal*, 21(3):243-245.

Watson, D. F., 1982. ACORD: Automatic Contouring of Raw Data. *Computers & Geosciences,* 8(1):97-101.